Extraction of Long-Chain Fatty Acids in Isolated Rat Heart During Acute Low-Flow Ischemia

Wolf-S. Richter, Steffen Fischer, Nicole Ernst, and Dieter L. Munz

Clinic for Nuclear Medicine, University Hospital Charité, Humboldt University of Berlin, Berlin, Germany

Although β-oxidation of fatty acids is suppressed rapidly during ischemia, the behavior of fatty acid extraction at different flow rates is incompletely understood. This study assessed the relationship between flow and extraction of ^{123}I-iodophenylpentadecanoic acid (IPPA) in the isolated heart model, especially at low flow. **Methods:** Isolated hearts from male Wistar rats (n = 15) were subjected to retrograde perfusion with constant flow (Krebs Henseleit solution containing 10 mmol/L glucose). A latex balloon in the left ventricle allowed isovolumetric contractions and ventricular pressure measurements. The extraction of ^{123}I-IPPA was assessed with the indicator dilution technique and ^{99m}Tc-albumin as the intravascular reference. The flow was either increased from the control flow (8 mL/min) until 300% or reduced until 10%. ^{123}I-IPPA extraction was measured three times before and 10 min after flow alteration. The tracer uptake was estimated from the product of net extraction and flow. **Results:** The mean ^{123}I-IPPA extraction at the control flow (third measurement) was 51.6% ± 2.8%. Between flow rates of approximately 25% and 300%, ^{123}I-IPPA extraction increased exponentially at decreasing flow rates. At flow rates ≤25% of the control flow, ^{123}I-IPPA extraction was exponentially higher than predicted. ^{123}I-IPPA uptake and flow changed largely in parallel. During low flow, the rate–pressure product showed the expected decline (perfusion–contraction matching). **Conclusion:** The extraction of ^{123}I-IPPA is preserved and slightly increased (relative to flow) during acute low-flow ischemia.

Key Words: ^{123}I-iodophenylpentadecanoic acid; myocardial metabolism; low-flow ischemia; fatty acid extraction

J Nucl Med 2001; 42:1101–1108

A sufficient amount of high-energy phosphates is a prerequisite for contractile function of the heart. In contrast to other organs, the heart can use all available substrates for energy production. In this regard, fatty acids are of special importance, because they are the substrate used primarily for oxidative metabolism (*1*).

The heart possesses only a limited capacity for the de novo synthesis of fatty acids. Therefore, the heart relies on the blood for the supply of fatty acids. The amount of fatty acids taken up by myocardial cells depends on fatty acid extraction and on regional myocardial blood flow. Information about fatty acid extraction in different pathophysiologic situations is limited, because most experimental studies assessed β-oxidation and not extraction. Furthermore, conflicting results have been obtained in different studies, showing both decreased and increased fatty acid uptake relative to flow (*1–4*). Therefore, this study analyzed in the isolated heart model the relationship between myocardial flow and the extraction of the long-chain fatty acid analog ^{123}I-iodophenylpentadecanoic acid (IPPA), especially at low flow, and obtained an estimate of ^{123}I-IPPA uptake at different flow rates.

MATERIALS AND METHODS

Preparation and Study Protocol

Male Wistar rats (weight range, 250–350 g) were anesthetized with sodium thiopental (15 mg/100 g of body weight intraperitoneally). The thorax was opened, and the heart was excised quickly, placed on ice-cold saline, and perfused retrogradely according to Langendorff after cannulation of the ascending aorta. Hearts were perfused at a constant flow with a nonrecirculating, modified Krebs–Henseleit solution containing (in mmol/L) NaCl (118), KCl (4.7), $CaCl_2$ (2.52), $MgSO_4$ (1.64), $NaHCO_3$ (24.88), KH_2PO_4 (1.18), and glucose (10) equilibrated with 5% CO_2/95% O_2 at 37°C. All chemicals and reagents were purchased from Sigma-Aldrich (Deisenhofen, Germany). Perfusate was filtered (0.2 μm) to prevent particulate matter from entering the coronary circulation. A latex balloon filled with water was introduced into the left ventricle and permitted continuous pressure measurements. The balloon volume was adjusted to obtain a left ventricular end-diastolic pressure of approximately 5 mm Hg.

The roller pump used for retrograde perfusion of the hearts was calibrated before each experiment by determining the pumped volume at different flow levels. During the experiments, the flow was altered by adjusting the roller pump, and the flow rates were controlled by collecting venous outflow from the heart. Measured flow rates and predetermined pumping rates were virtually identical (±0.1 mL).

After preparation, all hearts were perfused at a flow rate of 8 mL/min for 20 min without intervention (stabilization phase), and then ^{123}I-IPPA extraction was measured 3 times at 15-min intervals (baseline extraction). The flow rate of 8 mL/min resulted in a mean aortic pressure of approximately 40 mm Hg. Fifteen minutes after the third measurement, the flow was either reduced or increased, and ^{123}I-IPPA extraction was measured 10 min later at the altered flow rate. ^{123}I-IPPA extraction at the third baseline measurement

Received Oct. 28, 2000; revision accepted Mar. 5, 2001.

For correspondence or reprints contact: Wolf-S. Richter, MD, Clinic for Nuclear Medicine, University Hospital Charité, Schumannstr. 20/21, 10098 Berlin, Germany.

SOCIETY OF NUCLEAR MEDICINE

was used as the reference for the assessment of effects during intervention. Hearts were beating spontaneously during the whole experiment. At the end of the measurements, the hearts were cut into 4 or 5 coronal slices and stained with 2,3,5-triphenyltetrazolium chloride (tetrazolium red) (*5,6*). No heart showed macrosopic evidence of severe myocardial damage (unstained segments).

Analysis of Capillary ^{123}I-IPPA Exchange

^{123}I-IPPA extraction was measured according to the indicator dilution technique described elsewhere (*7–10*). A tracer bolus consisting of 100 kBq ^{123}I-IPPA (diffusible tracer) and 100 kBq ^{99m}Tc-albumin (vascular reference) was dissolved in 300 μL perfusate and added to the arterial inflow just above the heart. A special aortic cannula consisting of two parallel glass tubes was used for the bolus injection. By switching from one tube to the other, radiolabeled substances could be added to the perfusate without a change of flow rate (Fig. 1). To avoid adhesion of radiopharmaceuticals to the perfusion apparatus, any part coming into direct contact with ^{123}I-IPPA or ^{99m}Tc-albumin was made of glass and pretreated with a silicone solution (Sigmacote; Sigma-Aldrich, Deisenhofen, Germany).

Venous outflow was collected for a total of 5 min. At the flow rate of 8 mL/min, venous samples were obtained at 3, 6, 9, 12, 15, 20, 25, 30, 45, 60, 90, 120, 150, 200, 250, and 300 s. Sampling intervals were adapted to the flow rate during measurements at lower flow to guarantee a size of venous samples >200 μL (e.g., samples were obtained at 10, 20, 30, 45, 60, 90, 120, 150, 200, 250, and 300 s at a flow rate of 2 mL/min). Because multiple consecutive measurements were performed on each heart, one venous sample was obtained immediately before injection of every activity bolus, and subsequent samples were corrected for residual activity. Venous samples were counted on an automated γ-counter (1282 CompuGamma; Wallac, Turku, Finland). For discrimination of ^{99m}Tc and ^{123}I, energy windows were centered manually on the peaks of both isotopes, and results were corrected for energy crossover (6.5% downscatter of ^{123}I into the ^{99m}Tc window), time, background, and physical decay during the counting process. Each 100-μL sample was measured for 60 s, and the mean activity at the time of bolus passage was around 150,000 and 60,000 counts/min in the ^{99m}Tc and ^{123}I windows, respectively.

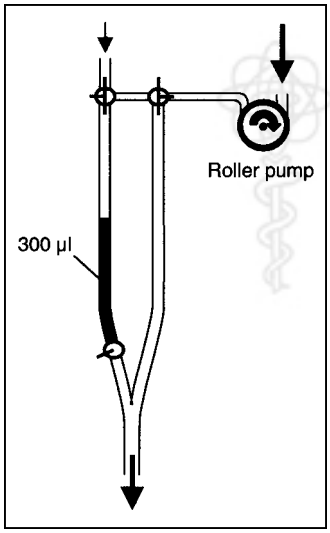

FIGURE 1. For application of tracer bolus at constant flow, special aortic cannula was used, which consisted of two parallel tubes. Arrows represent direction of flow. Tracer bolus of 300 μL was added to tube on left-hand side. By switching perfusion from one tube to the other, bolus was administered to heart at constant flow.

Normalized transport functions h(t) were calculated for ^{123}I-IPPA and ^{99m}Tc-albumin as follows:

$$h(t) = F\left(\frac{A(t)}{A_0}\right), \qquad \text{Eq. 1}$$

where F is the flow in milliliters per minute, A(t) is the radioactivity in disintegrations per minute (dpm) per milliliter at time t, and A_0 is the total injected activity in dpm. From the h(t) curves, an instantaneous extraction E(t) was obtained for each point:

$$E(t) = 1 - \frac{h(t)_{ippa}}{h(t)_{alb}}, \qquad \text{Eq. 2}$$

where $h(t)_{ippa}$ and $h(t)_{alb}$ are the normalized transport functions for ^{123}I-IPPA and ^{99m}Tc-albumin, respectively.

The Renkin–Crone equation (*11–13*) can be used to determine the capillary permeability–surface area product PS_c, given that PS_c represents a unidirectional flux:

$$PS_c = -F \ln(1 - E_{max}), \qquad \text{Eq. 3}$$

where E_{max} is the peak instantaneous extraction E(t) occurring up to the peak of $h(t)_{alb}$.

The net extraction $E_{net}(t)$, which reflects bidirectional tracer exchange, was calculated from the outflow curves as a time integral:

$$E_{net}(t) = \frac{\int_0^t [h(t)_{alb} - h(t)_{ippa}]d\lambda}{\int_0^t h(t)_{alb}d\lambda}, \qquad \text{Eq. 4}$$

where λ is a dummy variable for integration and t is the time at which 99% of the injected albumin activity had emerged in the venous effluent. From the outflow curves, residue fractions R(t) were calculated for ^{123}I-IPPA:

$$R(t) = 1 - \int_0^t h(\lambda)d\lambda. \qquad \text{Eq. 5}$$

Net tissue tracer uptake, which is a function of tracer delivery and E_{net}, was determined from the product of flow and E_{net}:

$$Uptake_{net} = F \times E_{net}. \qquad \text{Eq. 6}$$

For further analysis of tracer exchange over the capillary wall, time curves of the log ratio for ^{99m}Tc-albumin and ^{123}I-IPPA were generated: $\ln[(C_{alb}(t)/C_{ippa}(t)]$, where $C_{alb}(t)$ and $C_{ippa}(t)$ are the concentrations in the venous outflow of ^{99m}Tc-albumin and ^{123}I-IPPA, respectively.

Radiopharmaceuticals

^{123}I-IPPA was obtained from Cygne bv (Eindhoven, The Netherlands). According to the manufacturer's information, the specific activity of ^{123}I-IPPA at calibration was >0.17 GBq/mg, and the total amount of IPPA injected with each activity bolus was <2 ng

SOCIETY OF NUCLEAR MEDICINE

(radiochemical purity >95%). Before this study, we were able to ascertain in separate experiments that the saturation of myocardial ^{123}I-IPPA uptake does not occur at the doses and volumes used in this study. ^{99m}Tc-albumin was prepared from a commercially available kit (albumoscint; duPont Pharmaceuticals, Bad Homburg, Germany), and labeling efficiency was >98% in all preparations.

Left Ventricular Performance

The analog-to-digital conversion of signals from the pressure transducer connected to the latex balloon in the left ventricle was performed using a data acquisition card compatible with a personal computer (PCL-818HD; Advantech Co. Ltd., Cincinnati, OH) and a conversion rate of 1,000 Hz. Data were processed using dedicated software (DaisyLab; Datalog GmbH, Mönchengladbach, Germany). The left ventricular end-diastolic pressure (LVEDP), left ventricular end-systolic pressure (LVESP), and heart rate were obtained from the left ventricular pressure curve, and the difference between LVEDP and LVESP was calculated (left ventricular developed pressure [LVDP]). The product of the heart rate and LVDP served as an index of myocardial work (rate–pressure product). The measurements of the heart rate and LVDP were performed immediately before injection of every activity bolus.

Statistics

Data are given as the arithmetic mean ± SE. The differences between the groups were examined using the nonparametric Mann-Whitney test. Statistical significance was assumed for $P < 0.05$.

RESULTS

Fifteen hearts were examined. The number of hearts studied at specific flow rates during intervention is summarized in Table 1. The mean heart weight at the end of the experiments was 1.8 ± 0.06 g.

Measurements at Baseline

The net extraction of ^{123}I-IPPA did not change significantly during the baseline phase and was 50.8% ± 3.1% (first measurement), 48.8% ± 3.7% (second measurement), and 51.6% ± 2.8% (third measurement). At the time of the third measurement, the rate–pressure product was 12,000 ± 1,500 mm Hg/min, the PS_c product was 3.7 ± 0.24 mL/g · min, and the LVEDP was 7.2 ± 0.7 mm Hg.

TABLE 1
Number of Hearts Examined at Specific Flow Rates During Intervention

Flow rate during intervention*	*n*
10%–20%	2
20%–30%	8
50%	1
200%	2
300%	2

*Percentage baseline flow (8 mL/min).

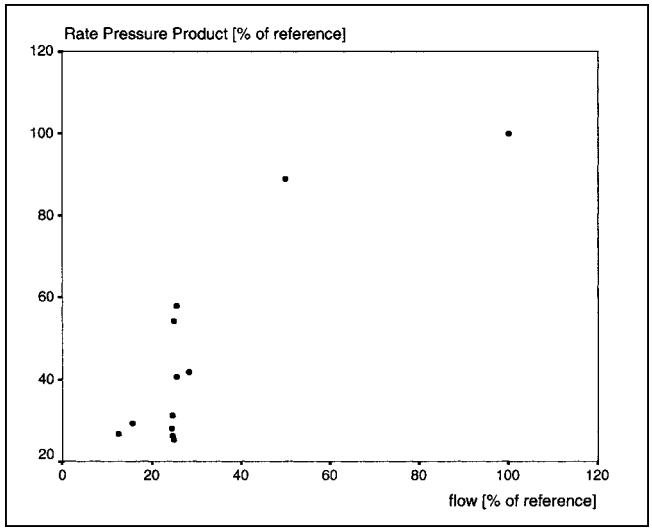

FIGURE 2. During flow reduction, rate–pressure product showed expected decline (perfusion–contraction matching).

Interventions

As predicted by the principles of perfusion–contraction matching (*14*), the rate–pressure product declined during low flow and remained constant at high flow (Fig. 2). The LVEDP did not change significantly during alteration of the flow. The PS_c product increased with increasing flow (Fig. 3).

^{123}I-IPPA net extraction increased during flow reduction and decreased at flow rates above the control flow. The relationship between flow and ^{123}I-IPPA extraction was exponential for flow rates between approximately 25% and 300% (flow percentages relative to the baseline flow). At flow rates ≤25% of the baseline, the increase in ^{123}I-IPPA extraction was greater than predicted by an exponential relationship in all hearts. Figure 4 shows a semilogarithmic

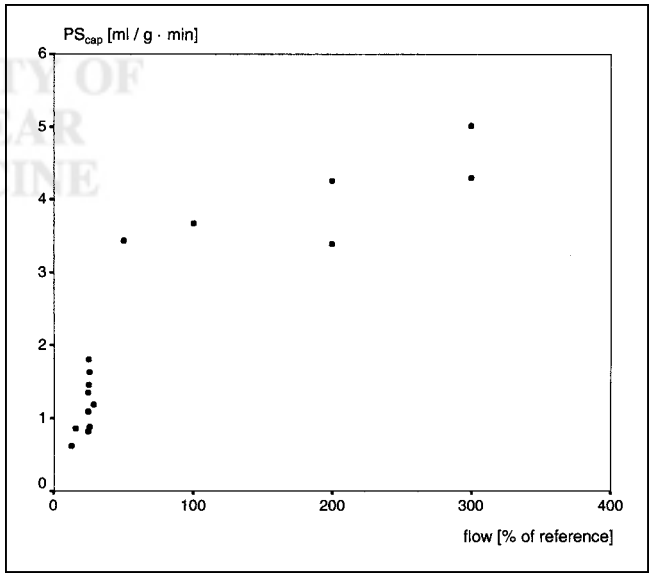

FIGURE 3. PS_c product increased with higher flows (recruitment of capillary surface).

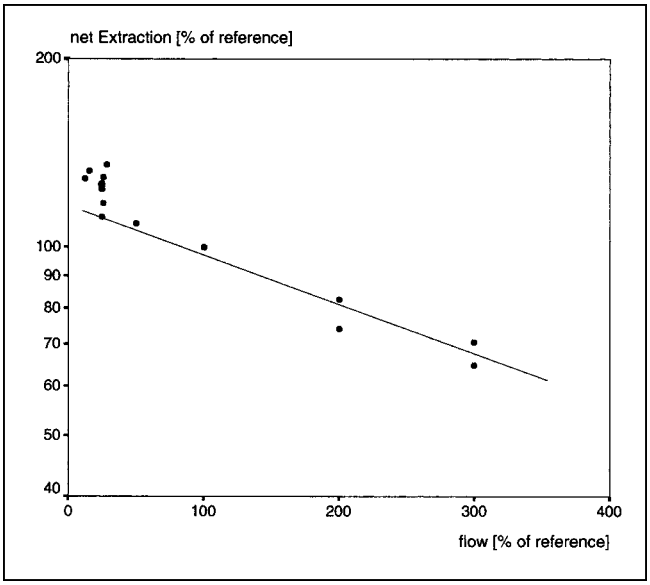

FIGURE 4. Semilogarithmic plot of net extraction and flow. Relationship between E_{net} and flow was exponential at flow rates between approximately 25% and 300% (inserted line). At lower flow rates, extraction was higher than predicted by exponential relationship.

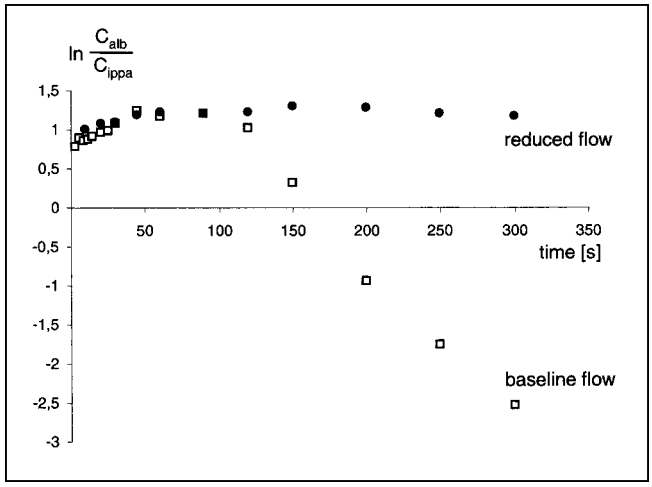

FIGURE 6. Log ratio–time plot for ^{123}I-IPPA at baseline flow (8 mL/min) and during flow reduction to 2 mL/min. First upward-sloping component reflects tracer that reaches outflow without transversing capillary walls. Second downward-sloping component is caused by return of label to intravascular space. Return of label from extravascular space was encountered only at baseline flow and could not be documented at flows ≤25% baseline. Inference is that tracer washout (backdiffusion) was limited at very low flows.

plot of ^{123}I-IPPA extraction versus flow. The solid line represents the regression for flow rates from approximately 25% to 300%.

The calculation of residue functions revealed higher ^{123}I-IPPA retention at low flows. An example is shown in Figure 5 for flows at the baseline and at 25% of the baseline.

Log ratio–time plots showed clear differences with varying flows (Fig. 6). In the log ratio–time plot, the early rising slope corresponds to material reaching outflow without transversing capillary walls, whereas the later downward deviation corresponds to the return to vasculature of the tracer that previously left capillaries (*15*). In Figure 6, a downward-sloping second component can be detected easily at the baseline flow, whereas the log ratio remained largely stable over time at a flow of 25% of the baseline.

The uptake of ^{123}I-IPPA increased with increasing flow. Figure 7 shows individual values together with the line representing the relationship between uptake and flow for an optimal perfusion tracer. At flow rates below the baseline,

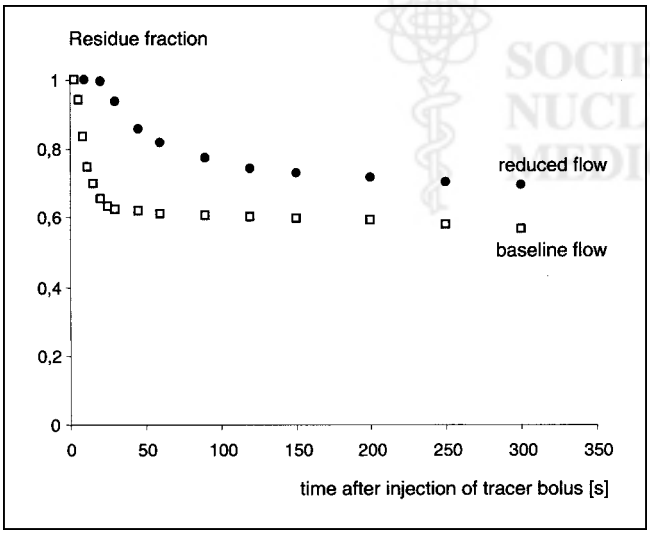

FIGURE 5. Residue fraction of ^{123}I-IPPA at baseline flow and at reduced flow (25% of baseline), calculated according to Equation 5. ^{123}I-IPPA retention increased at low flows.

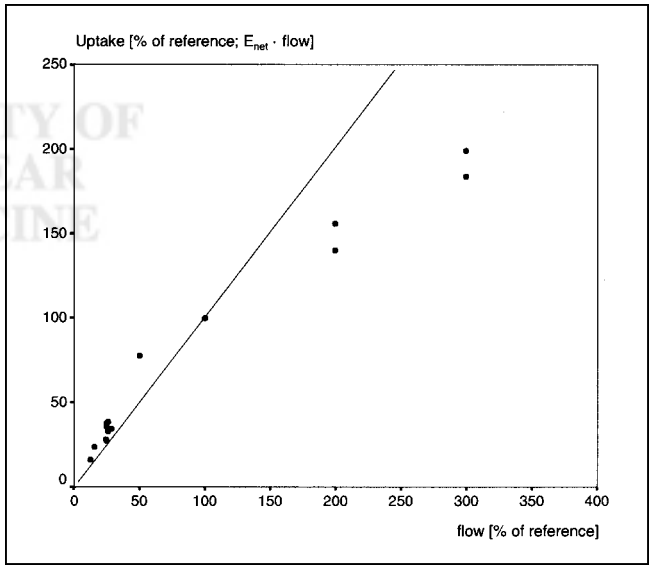

FIGURE 7. Plot of calculated ^{123}I-IPPA uptake (Eq. 6) vs. flow. Inserted line represents relationship between uptake and flow for optimal flow tracer (slope = 1). ^{123}I-IPPA uptake and flow changed largely in parallel.

SOCIETY OF NUCLEAR MEDICINE

all individual uptake values lie above this line; that is, ^{123}I-IPPA uptake was (slightly) higher than the flow. Conversely, the relative ^{123}I-IPPA uptake was less than the relative flow at high flow rates.

DISCUSSION

^{123}I-IPPA was developed by Machulla et al. (*16,17*) and used subsequently as an effective tracer of myocardial fatty acid metabolism. Its myocardial uptake depends on coronary perfusion (among other factors), and it undergoes β-oxidation (*18*). The myocardial kinetics of ^{123}I-IPPA are similar to the kinetics of the physiologic substrate palmitic acid (*19*). The advantages of ^{123}I-IPPA over labeled alkyl fatty acids are its rapid myocardial extraction, its stability against deiodination, and its rapid clearance of metabolites.

From ^{123}I-IPPA SPECT, the segmental tracer uptake and the half-lives of the biexponential myocardial clearance can be assessed. ^{123}I-IPPA uptake depends on regional myocardial blood flow and extraction. Detailed information about fatty acid extraction in different pathophysiologic situations is scarce. Instead of extraction, most studies dealing with myocardial metabolism examine the oxidation of different energy-yielding substrates and their contribution to adenosine triphosphate production. These studies showed that β-oxidation of fatty acids is rapidly inhibited during ischemia (*20*). In a canine open-chest model with flow reduction to 25% of the control flow, the consumption of nonesterified fatty acids dropped to 17% of the control conditions, whereas the oxidative and anaerobic metabolism of glucose more than tripled (*1*).

This study examined the relationship between flow and ^{123}I-IPPA net extraction. It was of special interest to assess whether the inhibition of β-oxidation during ischemia, as observed in previous studies, is associated with a decrease of fatty acid extraction. This study showed that the net extraction of ^{123}I-IPPA is preserved in myocardium subjected to global low flow and that extraction is even increased disproportionally at flows ≤25% of the control flow. The uptake of ^{123}I-IPPA increased slightly in comparison with an ideal flow tracer at low flow and seemed to plateau at high flow rates (>200% of the control flow).

Tracer extraction and regional blood flow are coupled. During low flow, the contact time of the labeled tracer with the capillary wall increases and extraction rises. The relationship between flow, permeability, and extraction is described by the Renkin–Crone equation, $E = 1 - e^{-PS/F}$, where E is extraction and F is flow. From the Renkin–Crone equation, an exponential relationship between flow and extraction can be assumed, at least in situations where the saturation of specific mechanisms for tracer transport does not occur.

Experimental results regarding the relationship between regional myocardial blood flow and the extraction of long-chain fatty acids are controversial. In an open-chest dog preparation, Myears et al. (*1*) measured the steady-state extraction fraction of nonesterified fatty acids (NEFA) in myocardium from the arteriovenous difference of plasma concentrations. They found a virtual identical (P = not significant) extraction fraction of NEFA at control conditions (41.2% ± 6.0%), during flow reduction to 25% of the control flow (36.6% ± 2.7%), and at reflow (42.6% ± 5.6%). In contrast, the extraction fraction of glucose increased significantly during ischemia from 2.2% ± 2.0% to 25.0% ± 2.0% and remained enhanced during reperfusion (15.4% ± 2.2%; $P < 0.05$ compared with control conditions and with ischemia).

Similarly, Schwaiger et al. (*2*), using a canine open-chest model with intracoronary injection of ^{11}C-palmitate and measurement of the retention fraction with a scintillation probe, found no change of palmitate retention during reduction of the epicardial flow to 29.4% of the control flow with simultaneous reduction of the endocardial flow to 10.7%.

At variance with the experimental findings of Myears et al. (*1*) and Schwaiger et al. (*2*) is the study of Vyska et al. (*3*), who determined ^{123}I-IPPA kinetics in 15 healthy patients and 30 patients with coronary artery disease. They calculated that k_1*, the rate constant for ^{123}I-IPPA influx into myocardial tissue, increased in a nonlinear fashion with reduction of the relative plasma flow rate. Likewise, Marie et al. (*4*) found an exponential increase of early ^{123}I-16-iodo-3-methylhexadecanoic acid (MIHA) retention with decreasing coronary flow rate in the isolated rabbit heart perfused with red cell–enhanced perfusate.

Also in this study, the net extraction of ^{123}I-IPPA increased with decreasing flow and even showed a more than proportional increase at flow rates ≤25% of the control flow. The findings of this study support the assumption that the extraction of ^{123}I-IPPA largely follows the principles of the Renkin–Crone equation. The apparent differences between this study and the results of Myears et al. (*1*) and Schwaiger et al. (*2*) may be explained by four factors. First, Myears et al. (*1*) calculated the extraction fraction of NEFA from arteriovenous differences in a steady-state situation. In contrast, in most other studies, a tracer bolus is injected (pulse-labeling technique). The distribution of the label in the intracellular lipid pools may be different with both techniques, and the calculated extraction fractions may vary. Second, Myears et al. (*1*) obtained venous blood from the vein draining the ischemic territory. Venous effluent may be diluted by blood from nonischemic regions, thus masking discrete alterations of NEFA extraction. Third, ^{123}I-IPPA and glucose (without insulin) were the only energy substrates in the Langendorff preparation used in this study. In the open-chest models used by Myears et al. (*1*) and Schwaiger et al. (*2*), competing substrates may have influenced fatty acid extraction. Fourth, Myears et al. (*1*), Schwaiger et al. (*2*), Vyska et al. (*3*), and Marie et al. (*4*) measured the extraction of different substrates (NEFA, ^{11}C-palmitate, ^{123}I-IPPA, and ^{123}I-MIHA). The studies examining ^{123}I-IPPA and ^{123}I-MIHA documented a flow dependency of influx/extraction. The different results may

therefore be caused by tracer-specific uptake and retention/metabolism. Tracer-specific differences of extraction have been documented for ^{18}F-fluoro-6-thiaheptadecanoic acid (FTHA) and ^{125}I-β-methyl-*p*-iodophenylpentadecanoic acid (^{125}I-BMIPP) in the hypoxic state (*21*). Similar information about ^{123}I-IPPA is lacking.

The calculation of residue functions and the analysis of log ratio–time plots can give insight into the mechanisms responsible for the more than proportional increase of net extraction at very low flow rates in this study. At flows ≤25% of the baseline, the residue functions showed an increased retention of ^{123}I-IPPA, whereas the log ratio–time plots showed almost no net washout (backdiffusion). The inference is that a limitation of tracer washout constitutes an important factor in the more than proportional increase of ^{123}I-IPPA net extraction at low flows. A partial limitation of tracer washout must be expected when the flow is lower than the PS_c product of the substance under investigation (*22*), which is clearly the case at the low flows produced in this study. Alternatively, the observed increase of ^{123}I-IPPA retention at low flows may also be caused by a more avid cellular extraction; however, the data of this study do not allow (but also do not rule out) this conclusion.

The calculated PS_c product of 3.7 ± 0.24 mL/g · min is in the range of published PS_c products for labeled palmitate (1.6 and 7.0 mL/g · min) (*15*,*23*) and higher than values for ^{201}Tl (between 0.7 ± 0.3 and 1.22 ± 0.4 mL/g · min) (*22*,*24*,*25*) and ^{99m}Tc-sestamibi (approximately 0.48 mL/g · min) (*24*). The increase of PS_c with flow can be explained theoretically by an increase in capillary permeability or capillary surface area (or both). This increase most likely reflects a recruitment of the capillary surface at higher flows, which has also been described for K^+ and Tl^+ (*22*,*25*).

In this study, ^{123}I-IPPA uptake was calculated from the product of flow and net extraction (Eq. 6). The calculated ^{123}I-IPPA uptake and flow changed largely in parallel. However, at low flow rates, the uptake of ^{123}I-IPPA increased slightly in comparison with flow and showed a tendency to plateau at high flow rates (>200% of the control flow). These results concerning uptake are in accordance with former studies. Schwaiger et al. (*26*) studied ^{11}C-palmitate uptake in a canine model with 3-h balloon occlusion of the left anterior descending coronary artery (LAD). Although the flow was reduced to 31.8% ± 10.6%, ^{11}C-palmitate uptake was reduced to 36.0% ± 11.0%. The relative decrease of ^{11}C-palmitate was paralleled by blood flow reduction ($r = 0.75$). Van der Vusse et al. (*27*) reported a reduced uptake of NEFA in ischemic canine myocardium produced by partial occlusion of the LAD for 120 min. Comparable with this study, NEFA uptake was slightly higher than flow. Renstrom et al. (*21*) studied ^{125}I-BMIPP and ^{18}F-FTHA uptake in 19 swine. During flow reduction to 40% of the control flow, the uptake of both tracers was reduced to approximately 60%.

Comans et al. (*28*) examined the uptake of ^{125}I-iodophenyl-3,3-dimethylpentadecanoic acid (DMIPP) in dogs with an extracorporally perfused LAD at different flow rates. The flow was determined with ^{46}Sc-labeled microspheres, and ^{125}I-DMIPP uptake was assessed as the percentage injected dose per gram. In their study, the relationship between normalized blood flow and normalized ^{125}I-DMIPP uptake could be best described by an exponential relationship with higher ^{125}I-DMIPP uptake than flow at lower flow rates (comparable with the results of this study).

Using the same model, Sloof et al. (*29*) studied the heterogeneity of blood flow and ^{125}I-DMIPP uptake at different flow rates. During flow reduction, the heterogeneity increased significantly for both myocardial blood flow and ^{125}I-DMIPP uptake, whereas the agreement between both parameters decreased. Sloof et al. (*29*) concluded that serious uncoupling occurs between fatty acid metabolism and myocardial blood flow during flow reduction. This study also showed a greater variability of rate–pressure products and net extraction at low flows (Figs. 2 and 4).

The clinical interpretation of myocardial SPECT depends mainly on the analysis of tracer uptake. In this regard, the uptake of fatty acids and flow tracers must be compared. It can be deduced from this study that during acute low-flow ischemia, the uptake of fatty acids and flow tracers will be reduced to a similar extent (probably slightly in favor of fatty acids). A similar situation may exist in chronic ischemia. In patient studies, a preserved (increased) uptake of fatty acids in chronically ischemic segments and chronically dysfunctional but viable myocardium could indeed be shown (*30*,*31*).

A different situation exists in myocardium studied after an ischemic event (acute coronary syndrome with reperfusion, exercise-induced ischemia). Different clinical studies have shown a reduced fatty acid uptake in comparison with flow in stunned myocardium (*32*,*33*).

Kudoh et al. (*34*) studied ^{123}I-BMIPP and ^{201}Tl uptake in 15 patients with chronic coronary artery disease and correlated tracer uptake with histologic findings of biopsy specimens obtained during cardiac surgery. Although early ^{201}Tl uptake (5–10 min after injection) showed a strong correlation with the degree of fibrosis, ^{123}I-BMIPP uptake was reduced disproportionally in segments with mild fibrosis (<15%) only. The findings of Kudoh et al. (*34*) most likely reflect a reduced fatty acid uptake in postischemic viable myocardium.

There were several limitations to this study. In this study, the whole heart was made ischemic. In contrast, myocardial perfusion in patients with coronary artery disease is characterized by regional inhomogeneities. The hemodynamic and metabolic consequences of global versus regional ischemia are probably different, and the results of this study are not directly transferable to the clinical situation.

The supply of energy-yielding substrates was controlled completely in the Langendorff model used. This is an advantage in one regard, because the effect of flow alterations

on fatty acid extraction could be studied separately. On the other hand, the use of energy substrates is balanced precisely in the physiologic situation, and, in previous studies, the uptake of fatty acids depended also on the availability of competing substrates (*35–38*). The effects of competing substrates in the low-flow situation were not examined here.

The perfusate in this study did not contain albumin or any oxygen carrier (e.g., red blood cells). To guarantee sufficient oxygen delivery to myocardial tissue, the flow rate was increased to 8 mL/min at the baseline. The combined effects of low oncotic pressure and low viscosity, compared with blood, together with the supraphysiologic flow rate, resulted in an aortic pressure of approximately 40 mm Hg at the baseline, which is in the range of published values for this model (*39*). The supraphysiologic flow rates may have affected individual measurements; however, the values obtained for E_{net} and PS_c at the baseline are comparable with results from other, more physiologic models. Furthermore, the relationship between flow and ^{123}I-IPPA extraction studied at different flow rates should be less prone to adverse effects from experimental conditions than the sole determination of individual data points.

The low oncotic pressure of the perfusate may have resulted in tissue edema with a concomitant increase in interstitial space, despite a relatively low perfusion pressure. The influence of tissue edema on the calculated parameters cannot be excluded, even if in separate experiments using the same model with a constant flow for >2 h, no time-dependent change of ^{123}I-IPPA extraction or PS_c could be detected.

This study examined adaptations to acute low-flow ischemia. Consequently, the results cannot be transferred directly to chronic low-flow ischemia (hibernation).

CONCLUSION

Fatty acid uptake is preserved and increased slightly, relative to flow, in low-flow ischemia. The analysis of ^{123}I-IPPA uptake gives insight into the subtle changes of cardiac energy metabolism, which may be of value for differential diagnosis and therapy monitoring in patients suffering from coronary artery disease.

ACKNOWLEDGMENTS

This study was supported in part by the internal research funding of Charité Medical School.

REFERENCES

1. Myears DW, Sobel BE, Bergmann SR. Substrate use in ischemic and reperfused canine myocardium: quantitative considerations. *Am J Physiol.* 1987;253:H107–H114.
2. Schwaiger M, Schelbert HR, Keen R, et al. Retention and clearance of C-11 palmitic acid in ischemic and reperfused canine myocardium. *J Am Coll Cardiol.* 1985;6:311–320.
3. Vyska K, Machulla HJ, Stremmel W, et al. Regional myocardial free fatty acid extraction in normal and ischemic myocardium. *Circulation.* 1988;78:1218–1233.
4. Marie PY, Menu P, Angioï M, et al. The kinetics of β-methyl-substituted labelled fatty acids in ischaemic myocardium: an analysis in man and with a blood-perfused isolated heart model. *Eur J Nucl Med.* 1999;26:474–482.
5. Kloner RA, Darsee JR, deBoer LW, Carlson N. Early pathologic detection of acute myocardial infarction. *Arch Pathol Lab Med.* 1981;105:403–406.
6. Greve G, Saetersdal T. Problems related to infarct size measurements in the rat heart. *Acta Anat Basel.* 1991;142:366–373.
7. Bassingthwaighte JB, Goresky CA. Modeling in the analysis of solute and water exchange in the microvasculature. In: Renkin EM, Michel CC, Geifer SR, eds. *Handbook of Physiology, Section 2: The Cardiovascular System*. Bethesda, MD: American Physiological Society; 1984:549–626.
8. Rose CP, Goresky CA. Interactions between capillary exchange, cellular entry, and metabolic sequestration processes in the heart. In: Renkin EM, Michel CC, Geifer SR, eds. *Handbook of Physiology, Section 2: The Cardiovascular System*. Bethesda, MD: American Physiological Society; 1984:781–798.
9. Bassingthwaighte JB, Chinard FP, Crone C, et al. Terminology for mass transport and exchange. *Am J Physiol.* 1986;250:H539–H545.
10. Meerdink DJ, Leppo JA. Experimental studies of the physiologic properties of technetium-99m agents: myocardial transport of perfusion agents. *Am J Cardiol*. 1990;66:9E–15E.
11. Crone C. The permeability of capillaries in various organs as determined by use of indicator diffusion method. *Acta Physiol Scand*. 1963;58:292–305.
12. Renkin EM. Transport of potassium-42 from blood to tissue in isolated mammalian skeletal muscles. *Am J Physiol*. 1959;197:1205–1210.
13. Renkin EM. Exchangeability of tissue potassium in skeletal muscle. *Am J Physiol.* 1959;197:1211–1215.
14. Ross JR Jr. Myocardial perfusion-contraction matching: implications for coronary heart disease and hibernation. *Circulation*. 1991;83:1076–1083.
15. Rose CP, Goresky CA. Constraints on the uptake of labeled palmitate by the heart: the barriers at the capillary and sarcolemmal surfaces and the control of intracellular sequestration. *Circ Res*. 1977;41:534–545.
16. Machulla HJ, Stöcklin G, Kupfernagel C, et al. Comparative evaluation of fatty acids labelled with ^{11}C, ^{34m}Cl, ^{77}Br and ^{123}I for metabolic studies of the myocardium. *J Nucl Med*. 1978;19:298–302.
17. Machulla H, Marsmann M, Dutschka K. Biochemical concept and synthesis of radioiodinated phenyl fatty acid for in vivo metabolic studies of the myocardium. *Eur J Nucl Med.* 1980;5:171–173.
18. Caldwell JH, Martin GV, Link JM, Krohn KA, Bassingthwaighte JB. Iodophenylpentadecanoic acid-myocardial blood flow relationship during maximal exercise with coronary occlusion. *J Nucl Med*. 1990;31:99–105.
19. Reske SN, Sauer W, Machulla HJ, Winkler C. 15-(*p*-I-123)phenyl pentadecanoic acid as a tracer of lipid metabolism: comparison with 1-C-14 palmitic acid in murine tissues. *J Nucl Med*. 1984;25:1335–1342.
20. van der Vusse GJ, Glatz JFC, Stam HCG, Reneman RS. Fatty acid homeostasis in the normoxic and ischemic heart. *Physiol Rev*. 1992;72:881–940.
21. Renstrom B, Rommelfanger S, Stone CK, et al. Comparison of fatty acid tracers FTHA and BMIPP during myocardial ischemia and hypoxia. *J Nucl Med.* 1998;39:1684–1689.
22. Bassingthwaighte JB, Winkler B, King RB. Potassium and thallium uptake in dog myocardium. *J Nucl Med.* 1997;38:264–274.
23. Goresky CA, Stremmel W, Rose CP, et al. The capillary transport system for free fatty acids in the heart. *Circ Res.* 1994;74:1015–1026.
24. Meerdink DJ, Leppo JA. Comparison of hypoxia and ouabain effects on the myocardial uptake kinetics of technetium-99m hexakis 2-methoxyisobutyl isonitrile and thallium-201. *J Nucl Med*. 1989;30:1500–1506.
25. Leppo JA, Meerdink DJ. Comparative myocardial extraction of two technetium-labeled BATO derivatives (SQ30217, SQ32014) and thallium. *J Nucl Med.* 1990;31:67–74.
26. Schwaiger M, Schelbert HR, Ellison D, et al. Sustained regional abnormalities in cardiac metabolism after transient ischemia in the chronic dog model. *J Am Coll Cardiol*. 1985;6:336–347.
27. van der Vusse GJ, Roemen THM, Prinzen FW, Coumans WA, Reneman RS. Uptake and tissue content of fatty acids in dog myocardium under normoxic and ischemic conditions. *Circ Res.* 1982;50:538–546.
28. Comans EFI, Visser FC, van Lingen A, et al. Exponential relationship between DMIPP uptake and blood flow in normal and ischemic canine myocardium. *Nuklearmedizin.* 1998;37:S54–S59.
29. Sloof GW, Visser FC, Comans EFI, et al. Heterogeneity of DMIPP uptake and its relationship with heterogeneous myocardial blood flow. *J Nucl Med.* 1997;38:1424–1430.
30. Sloof GW, Visser FC, Bax JJ, et al. Increased uptake of iodine-123-BMIPP in chronic ischemic heart disease: comparison with fluorine-18-FDG SPECT. *J Nucl Med*. 1998;39:255–260.
31. Mäki MT, Haaparanta MT, Luotolathi MS, et al. Fatty acid uptake is preserved

in chronically dysfunctional but viable myocardium. *Am J Physiol*. 1997;273: H2473–H2480.
32. Franken PR, de Geeter F, Dendale P, Demoor D, Block P, Bossuyt A. Abnormal free fatty acid uptake in subacute myocardial infarction after coronary thrombolysis: correlation with wall motion and inotropic reserve. *J Nucl Med.* 1994;35: 1758–1765.
33. Richter WS, Beckmann S, Cordes M, Schuppenhauer T, Schartl M, Munz DL. Combined thallium-201 and dynamic iodine-123 iodophenylpentadecanoic acid single-photon emission computed tomography in patients after acute myocardial infarction with effective reperfusion. *Clin Cardiol.* 2000;23:902–908.
34. Kudoh T, Tadamura E, Tamaki N, et al. Iodinated free fatty acid and Tl-201 uptake in chronically hypoperfused myocardium: histologic correlation study. *J Nucl Med.* 2000;41:293–296.
35. Randle PJ, Garland PB, Hales CN, Newsholme EA. The glucose-fatty acid cycle: its role in insulin sensitivity and the metabolic disturbances of diabetes mellitus. *Lancet.* 1963;1:785–789.
36. Nuutila P, Koivisto VA, Knuuti J, et al. Glucose-free fatty acid cycle operates in human heart and skeletal muscle in vivo. *J Clin Invest.* 1992;89:1767–1774.
37. Goodwin GW, Arteaga JR, Taegtmeyer H. Glycogen turnover in the isolated working rat heart. *J Biol Chem.* 1995;270:9234–9240.
38. Wolfe RR. Metabolic interactions between glucose and fatty acids in humans. *Am J Clin Nutr*. 1998;67(suppl):519S–526S.
39. Döring HJ, Dehnert H. The isolated perfused heart of warm-blooded animals according to Langendorff. *Methods of Experimental Physiology and Pharmacology (Technique of Biological Measurements, No. 5)* [in German]. 1st ed. March, Germany: Biomesstechnik-Verlag; 1985.

SOCIETY OF NUCLEAR MEDICINE